nature genetics

Mutations in voltage-gated potassium channel KCNC3 cause degenerative and developmental central nervous system phenotypes

Michael F Waters[1,2], Natali A Minassian[3], Giovanni Stevanin[4], Karla P Figueroa[1], John P A Bannister[3], Dagmar Nolte[5], Allan F Mock[3], Virgilio Gerald H Evidente[6], Dominic B Fee[7], Ulrich Müller[5], Alexandra Dürr[4], Alexis Brice[4], Diane M Papazian[3] & Stefan M Pulst[1,2,8]

Potassium channel mutations have been described in episodic neurological diseases[1]. We report that K^+ channel mutations cause disease phenotypes with neurodevelopmental and neurodegenerative features. In a Filipino adult-onset ataxia pedigree, the causative gene maps to 19q13, overlapping the SCA13 disease locus described in a French pedigree with childhood-onset ataxia and cognitive delay[2]. This region contains *KCNC3* (also known as *Kv3.3*), encoding a voltage-gated *Shaw* channel with enriched cerebellar expression[3]. Sequencing revealed two missense mutations, both of which alter *KCNC3* function in *Xenopus laevis* expression systems. $KCNC3^{R420H}$, located in the voltage-sensing domain[4], had no channel activity when expressed alone and had a dominant-negative effect when co-expressed with the wild-type channel. $KCNC3^{F448L}$ shifted the activation curve in the negative direction and slowed channel closing. Thus, $KCNC3^{R420H}$ and $KCNC3^{F448L}$ are expected to change the output characteristics of fast-spiking cerebellar neurons, in which KCNC channels confer capacity for high-frequency firing. Our results establish a role for KCNC3 in phenotypes ranging from developmental disorders to adult-onset neurodegeneration and suggest voltage-gated K^+ channels as candidates for additional neurodegenerative diseases.

Dominant spinocerebellar ataxias (SCA) are heterogeneous neurological diseases with phenotypes consisting of cerebellar ataxia, extrapyramidal signs, dysarthria, oculomotor abnormalities, motor neuron signs, cognitive decline, epilepsy, autonomic dysfunction, sensory deficits and psychiatric manifestations[5,6]. Twenty-six SCA loci have been described, and for ten, the causative gene or mutation has been determined. Little is known about the normal function of most SCA genes, although the majority represent polyglutamine (polyQ) expansion diseases.

We previously characterized a three-generation Filipino family (**Supplementary Fig. 1** online) segregating an adult-onset dominant ataxia[7] and having prominent cerebellar signs and symptoms and cerebellar atrophy on magnetic resonance imaging (**Fig. 1**). The clinical and imaging phenotypes were consistent with a degenerative SCA. A genome-wide linkage scan showed a disease locus in a ~4-cM region of 19q13, with a 3.89 multipoint LOD score (**Supplementary Fig. 1**). This region partially overlapped the *SCA13* locus[2] mapped in a French pedigree with mild mental retardation, early-onset ataxia and slow progression. Through high-resolution genetic mapping, the candidate region was further reduced in the Filipino pedigree. Haplotypes are shown in **Supplementary Figure 1**. Obligate recombinants were detected for both D19SMF1 (55.44 Mb) and D19S553 (56.24 Mb), defining an ~800-kb physical candidate region with the LOD-1 drop interval providing a probable location of the disease gene near D19S246 (55.64 Mb, LOD = 3.8, 95% penetrance; **Supplementary Fig. 1**).

This region contains approximately forty genes. At least four (synaptotagmin III (*SHANK1*), transcription factor Spi-B (*SPIB*), DNA polymerase delta subunit 125 (*POLD1*), and *KCNC3*) are expressed in the brain. Although the KCNC3 knockout mouse did not demonstrate marked signs of abnormal development or neurodegeneration, we focused on this gene, given its expression in Purkinje neurons. We identified two sequence changes in the S4 and S5 transmembrane segments encoded by exon 2: 1554G→A ($KCNC3^{R420H}$) in the Filipino pedigree (**Fig. 2a**) and 1639C→A ($KCNC3^{F448L}$) in the French pedigree (**Fig. 2b**). The mutations change amino acids that are 100% conserved among members of the human KCNC family and across phyla in the S4 and S5 domains (**Fig. 2c**,**d**).

[1]Division of Neurology and Rose Moss Laboratory for Parkinson's and Neurodegenerative Diseases, Burns and Allen Research Institute, Cedars-Sinai Medical Center, Los Angeles, California, 90048 USA. [2]Departments of Medicine and [3]Physiology, David Geffen School of Medicine at the University of California, Los Angeles (UCLA), Los Angeles, California, 90024 USA. [4]INSERM U679 and Department of Genetics, Cytogenetics, and Embryology of Assistance Publique - Hopitaux de Paris, Hôpital de la Salpêtrière, 75013 Paris, France. [5]Institut für Humangenetik, Justus-Liebig-Universität, 35392 Giessen, Germany. [6]Department of Neurology, Mayo Clinic, Scottsdale, Arizona 85259 USA. [7]Department of Neurology, University of Kentucky College of Medicine, Lexington, Kentucky 40536 USA. [8]Department of Neurobiology, David Geffen School of Medicine at UCLA, Los Angeles, California 90095 USA. Correspondence should be addressed to S.M.P. (stefan.pulst@cshs.org).

Received 7 November 2005; accepted 1 January 2006; published online 26 February 2006; doi:10.1038/ng1758

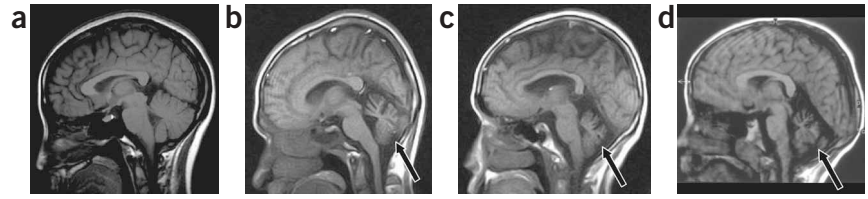

Figure 1 Mid-sagittal T1 sequence MR images. Shown are a normal control (**a**), individuals III-2 (**b**) and II-1 (**c**) of the Filipino pedigree and a 5-year-old individual from the French pedigree[2] (**d**). Affected individuals show marked cerebellar volume loss (arrows). Duration of disease is 43 years in individual II-1 (age 65 at imaging) and 4 years in III-2 (age 30 at imaging), which is likely to account for the more pronounced degeneration in II-1.

The mutations were seen in all affected individuals but not in unaffected individuals in the respective pedigrees. Additionally, the mutations were not found in over four hundred alleles from normal individuals of Filipino or Western European descent (data not shown).

Among voltage-gated K^+ channels, the functional properties of Kv3 channels are distinct. Kv3 channels activate in a more depolarized range and close much more rapidly than other Kv channels[8]. These properties facilitate high-frequency firing of action potentials with little or no adaptation, a characteristic of burst neuron populations found in the mammalian neocortex, hippocampus, auditory nuclei, substantia nigra and cerebellum[8]. Like other voltage-gated K^+ channels, Kv3 channels are tetramers. Different *Shaw* family subunits are able to assemble with each other, although not with subunits from other Kv subfamilies[9]. Each subunit has six transmembrane segments and a re-entrant loop (**Fig. 2c**). The first four transmembrane segments, S1–S4, constitute the voltage sensor domain, whereas the last two segments, S5 and S6, and the re-entrant loop form the ion-selective pore[10]. The depolarized voltage dependence and rapid deactivation that are characteristic of Kv3 channels are related properties conferred by specific amino acid residues in the voltage sensor and S5 (refs. 11,12). The Filipino mutation is located in S4 (**Fig. 2c**), the main voltage-sensing element, and changes one of the positively charged arginine residues that respond to changes in membrane potential[8,13]. The French mutation is at the cytoplasmic end of S5 (**Fig. 2c**), which is involved in coupling voltage sensor conformational changes with opening and closing of the pore[11]. F448L makes the properties of KCNC3 more similar to those of *Shaker* and other channels that normally have a leucine residue in the analogous position (**Fig. 2d**).

To investigate the functional consequences of the *SCA13* mutations, we expressed wild-type and mutant *KCNC3* alleles in *X. laevis* oocytes and recorded channel activity using a two-electrode voltage clamp. Activation of the wild-type KCNC3 channel was detected at –10 mV and more positive potentials (**Fig. 3a**). Upon repolarization to –90 mV, the channel closed quickly. In contrast, expression of R420H resulted in no detectable channel activity (**Fig. 3a**). Coexpression of wild-type KCNC3 and R420H subunits led to suppression of current amplitude consistent with a dominant-negative effect (**Fig. 3b**). R420H did not suppress the functional expression of *Shaker*, a member of the Kv1 (KCNA1) family (**Fig. 3b**). These results indicate that Kv3 subfamily–specific coassembly of wild-type and mutant subunits produces nonfunctional channels.

Expression of F448L produced channels with altered gating. Activation of F448L was detected at –20 mV, compared with –10 mV for the wild-type (**Fig. 4a**). Analysis of the probability of opening as a function of voltage confirmed that activation was shifted ~13 mV toward the hyperpolarized direction (**Fig. 4b**). Activation kinetics of F448L and wild-type were similar at voltages at which both have a maximal open probability (**Fig. 4c**). However, deactivation kinetics of F448L were markedly slower. Tail currents were recorded after repolarization to –90 mV using an 89 mM Rb^+ bath solution and were fitted with a single exponential component (**Fig. 4d**). This demonstrated a roughly sevenfold slowing of channel closure in F448L mutants. F448L mutation also slowed the rate of closing measured using a high K^+ bath solution (data not shown). The hyperpolarized

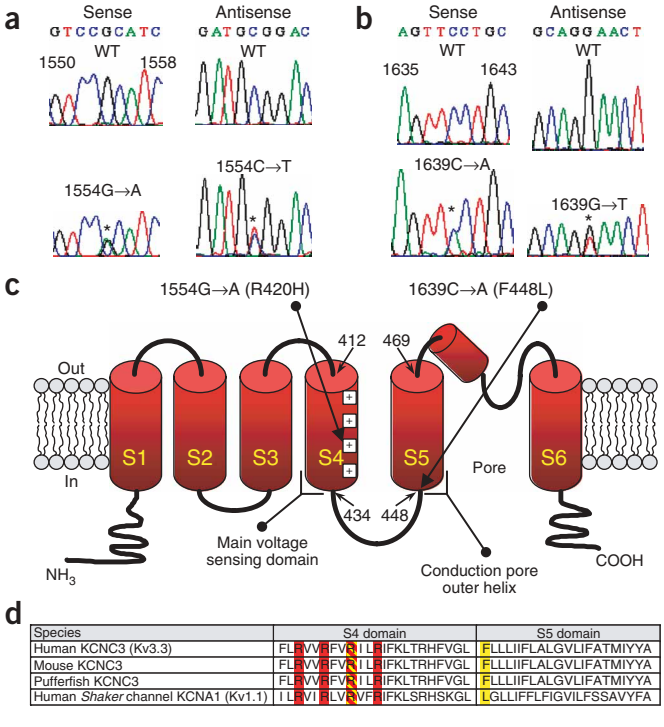

Figure 2 KCNC3 DNA mutations lead to amino acid substitutions in highly conserved domains. DNA sequence analysis shows the *KCNC3*^{R420H} 1554G→A (**a**) and *KCNC3*^{F448L} 1639C→A (**b**) point mutations in exon 2 of *KCNC3* (*Kv3.3*) that cause SCA13. Both sense and antisense strands are shown, as well as the wild-type (WT) sequence. Mutations are designated with an asterisk. (**c**) Functional motif schematic of a single KCNC3 subunit illustrating the six transmembrane segments and pore re-entrant loop (6TM architecture). Segments S1–S4 form the voltage sensor domain. Positively charged arginine residues in S4 detect changes in voltage. Segments S5 and S6 and the re-entrant loop form the ion-selective pore. S5 forms the pore outer helix and functions to couple voltage sensor conformational changes with pore opening and closing. Numbers indicate beginning and ending amino acids of S4 and S5 domains. Locations of SCA13 mutations are designated with arrows. (**d**) Amino acid sequence comparison of *Shaw* subfamily voltage-gated potassium channel across species demonstrates 100% conservation in S4 and S5 functional domains. The R420H (S4) and F448L (S5) mutations are highlighted in yellow. The positively charged arginine residues occurring every third position in segment S4 are highlighted in red. The final row shows a human *Shaker* channel sequence. The F448L mutation functionally converts KCNC3 into a *Shaker*-like channel.

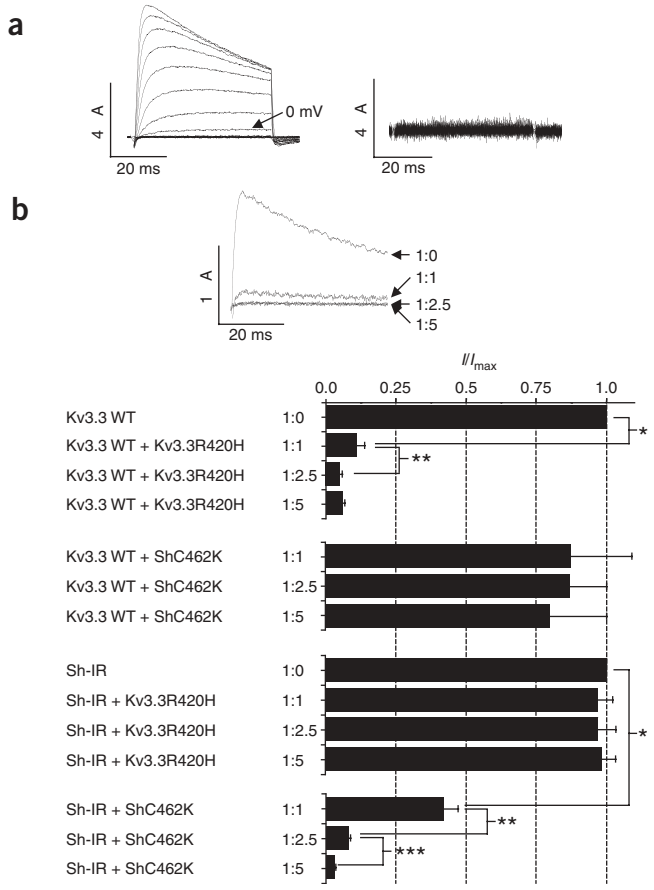

Figure 3 Subfamily-specific dominant-negative effect of R420H. (**a**) Current traces from wild-type (left) and R420H (right) channels were evoked by stepping from –90 mV to voltages ranging from –80 to +70 mV in 10-mV increments. In wild-type, partial inactivation was observed at potentials greater than +20 mV. The 0 mV record from wild-type channels is labeled for comparison with **Figure 4a**. (**b**) Top: representative current traces evoked by stepping from –90 mV to +60 mV for wild-type Kv3.3 expressed alone (1:0) or in the presence of R420H at the indicated ratios. Below: normalized peak current amplitudes at +60 mV for Kv3.3 wild-type expressed alone (1:0) or expressed with Kv3.3-R420H or Shaker-C462K (Sh-C462K, a non-functional Shaker subunit[30]) at the indicated ratios. Also shown are peak current amplitudes at +60 mV for inactivation-removed Shaker (Sh-IR) expressed alone (1:0) or expressed with Kv3.3-R420H or Sh-C462K at the indicated ratios. Values are provided as mean ± s.e.m., $n = 4$–10. Statistical significance was tested by one-way analysis of variance (ANOVA). $P < 0.05$: *, significantly different from 1:0; **, significantly different from 1:1; ***, significantly different from 1:2.5.

shift in the probability of opening and the slower rate of deactivation are related findings indicating that F448L increases the relative stability of the open state.

Unlike other genes implicated in spinocerebellar ataxias, the physiological functions of Kv3 channels in the cerebellum have been extensively studied and are reasonably well understood[14–17]. KCNC3 is expressed in cerebellar granule cells, Purkinje cells and deep cerebellar neurons, where it may form heteromultimeric channels by assembling with KCNC1 (Kv3.1) and/or KCNC4 (Kv3.4)[18,19]. In Purkinje cells, Kv3 channels are involved in repolarizing both somatic Na^+ spikes and dendritic Ca^{2+} spikes[17]. Kv3 channels are essential for fast spiking in burst neurons that fire hundreds of action potentials per second with little or no frequency adaptation[8]. Because of their depolarized activation range, Kv3 channels open only during action potentials, contribute to fast repolarization and thus promote recovery of Na^+ channels from inactivation. Fast deactivation of Kv3 channels limits the time course of the after-hyperpolarization, thereby shortening the refractory period.

It is likely that the SCA13 mutations disrupt the firing properties of fast-spiking cerebellar neurons and may influence neuronal function in additional regions of KCNC3 expression. Although the Kv3.3 knockout mouse has no obvious motor phenotype, the double Kv3.1/Kv3.3 knockout has marked symptoms, including tremor and severe ataxia[20]. Because R420H is expected to suppress the functional expression of KCNC3 as well as other subunits in the Kv3 family, this mutation may be more comparable to the double knockout. Pharmacological suppression of KCNC3 activity in cerebellar neurons leads to action potential broadening, spike frequency adaptation and spike failure from accumulated Na^+ channel inactivation[17]. R420H may have a similar effect. In contrast, F448L is predicted to reduce the maximal firing rate of cerebellar neurons. Owing to slower closing, after-hyperpolarization would be prolonged, thus delaying the return to threshold and increasing the interspike interval. The differing effects of the mutations at the cellular level may portend the contrasting phenotypes between the two pedigrees. The F448L mutation would be expected to be more severe because it alters key gating properties of Kv3 channels. In contrast, R420H would be expected to reduce channel activity without changing the functional properties of the residual current. The childhood onset with concurrent mental retardation and seizures in affected individuals of the French pedigree but the absence of these features in the Filipino patients is consistent with this notion.

The physiological properties of Kv3 channels provide tantalizing clues for potential mechanisms of neurodegeneration. Kv3 channels contribute substantially to the repolarization of both somatic Na^+ spikes and dendritic Ca^{2+} spikes in Purkinje cells[17]. Longer duration spikes would increase Ca^{2+} influx, which may contribute to neuronal death. Additionally, the functional properties of KCNC3 and KCNC4 channels are modulated by reactive oxygen species, and mutant KCNC3 subunits may affect the ability of cerebellar neurons to cope with oxidative stress[21–23]. Finally, morphological differentiation and the development of hallmark electrical properties are tightly linked in Purkinje cells. This raises the possibility that morphological and electrical maturation are interdependent phenomena[24]. Mutations that disrupt acquisition of appropriate electrical characteristics may cause subtle developmental defects that reduce the long-term viability of neurons.

Our results identify *KCNC3* mutations as causative of SCA13 and point to the importance of voltage-gated potassium channels in phenotypes ranging from developmental disorders to late-onset neurodegenerative disease. It is probable that *in vivo* model systems will be required to assess the consequences of mutant *KCNC3* on three distinct but interrelated functions: cerebellar development, cerebellar function in the mature organism and the role of proper channel function in preventing neuronal death. Both mutations show some intrafamilial phenotypic variability, highlighting the importance of compensatory mechanisms and the likely presence of other genetic and environmental modifiers.

Although no human disease has previously been associated with *KCNC3* variants, several reports demonstrate alterations in the expression patterns of potassium channels in Huntington, Parkinson and

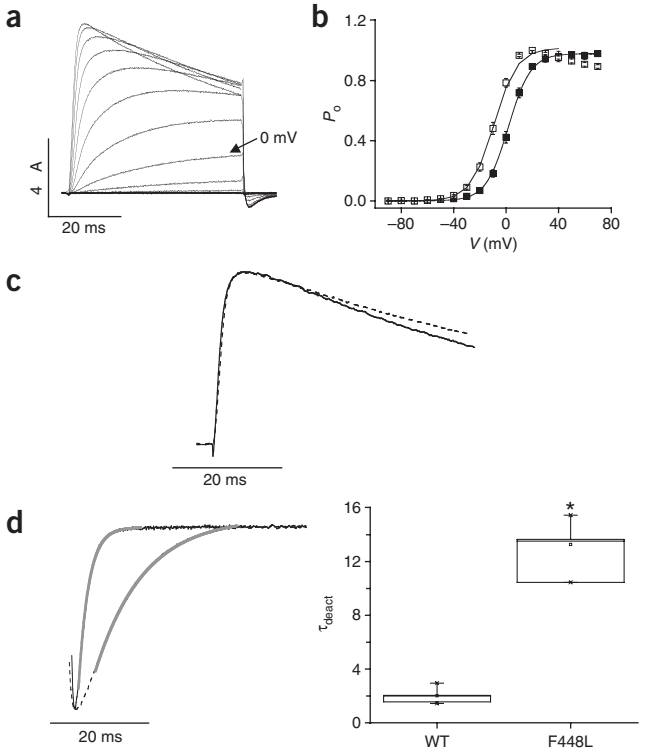

Figure 4 Altered gating in F448L. (**a**) Current traces from F448L channels were evoked by stepping from –90 mV to voltages ranging from –80 to +70 mV in 10-mV increments. The 0 mV record is labeled for comparison with **Figure 3a**. (**b**) To determine the probability of opening (P_o) as a function of voltage, wild-type or F448L currents were evoked by stepping from –90 mV to various test potentials, followed by repolarization to –90 mV. The bath solution contained 89 mM Rb^+. Isochronal tail current amplitudes were normalized to the maximal value obtained in the experiment and plotted against test potential. Filled squares: wild-type; open squares, F448L. Values are given as mean ± s.e.m., $n = 7$ (F448L) or 8 (wild-type). The data sets were fitted with single Boltzmann functions (solid lines), which yielded midpoint voltages of 2.8 ± 1.0 mV and –9.6 ± 1.3 mV and slope factors of 7.6 ± 0.3 and 7.6 ± 0.1 for wild-type and F448L channels, respectively. Midpoint voltages were significantly different ($P < 0.05$, Student's *t*-test). (**c**) Representative current traces obtained at +60 mV, scaled and overlaid for wild-type (solid line) and F448L (dashed line). (**d**) Left: representative tail currents from wild-type (solid line) and F448L (dashed line) recorded in an 89 mM Rb^+ bath solution, obtained by stepping from +10 to –90 mV. Traces have been scaled and overlaid. Tail currents were fit with a single exponential function (solid lines) to obtain values for the deactivation time constant, τ_{deact}. Right: box plot of τ_{deact} for wild-type and F448L. Mean values ± s.e.m. were 2 ± 0.2 ms and 13.3 ± 1.0 ms for wild-type ($n = 7$) and F448L ($n = 4$), respectively. Values of τ_{deact} differed significantly (one-way ANOVA; *, $P < 0.05$).

Alzheimer diseases[25–27]. The discovery of causative mutations in a voltage-gated K^+ channel now provides conclusive evidence for a role for these channels in neurodegeneration. The neurodegeneration field has been dominated by the hypothesis of misfolded proteins and their aggregation. The identification of *KCNC3* mutations and their functional characterization represent an additional avenue for understanding neuronal death. Recent neurophysiological studies of bursting neurons have led to the speculation that voltage-gated K^+ channels may be involved in human neurodegenerative disease. Our findings demonstrate that mutations in the Kv3 family of channels, which are important for the properties of bursting neurons, are sufficient to cause neurodegeneration. In addition, our results suggest that these channels be examined as mutational and therapeutic targets in bursting neurons in the hippocampus and substantia nigra, especially in conjunction with neurodegenerative diseases such as Parkinson and Alzheimer disease.

METHODS

Subjects. A Filipino family segregating a dominant trait for cerebellar ataxia was examined. There are eleven affected individuals including the proband, seven individuals in generation two and three individuals in generation three. In addition, there are five unaffected individuals in generation two, with one unaffected and 19 at-risk individuals in generation three. Blood was collected and DNA extracted from fifteen family members after informed consent was obtained. Institutional Review Board approval was obtained from Mayo Clinic and Cedars Sinai Medical Center.

Mutation and linkage analyses. To further evaluate linkage in the 19q13 region, additional markers were typed in the proband, seven affected individuals and four unaffected individuals in generation two, and three affected individuals in generation three. High-resolution mapping was performed by PCR amplification of dinucleotide repeat markers obtained in the region of 19q13 from the Ensembl genome browser (release 31.35d). Marker MF1 was amplified using the primer sequences in **Supplementary Table 1** and an annealing temperature of 55 °C. The PCR products were analyzed by electrophoresis on a 6% denaturing polyacrylamide gel.

Sequence analysis. DNA sequencing was performed using the ABI BigDye Terminator v3.1 cycle sequencing kit and the following protocol: to 5 ng (5 µl) purified PCR amplicon, 4 µl reaction pre-mix, 2 µl 5× sequencing buffer, 3.2 pmol (2 µl) appropriate primer and 7 µl deionized water were added in a 96-well microtiter plate. The plate was transferred to a PCR thermocycler (MJ Research PTC-200) and cycled as follows: 96 °C for 1 min followed by 25 cycles at 96 °C for 10 s, 50 °C for 5 s and 60 °C for 4 min. Sequencing products were then purified using ABI Centri-Sep spin columns. Resuspended samples were then electrophoresed on a 4.5% acrylamide gel in an ABI 377 DNA sequencer, according to the manufacturer's protocol. All sequences were analyzed using the BioEdit biological sequence alignment editor (v 5.0.9.1; Tom Hall, Isis Pharmaceuticals).

Electrophysiology. A human Kv3.3 cDNA clone was provided by James L. Rae (Mayo Foundation, Rochester, Minnesota)[28]. The coding region was transferred into the Bluescript II SK vector. Mutations were generated using the QuikChange method (Stratagene). RNA was transcribed and injected into *X. laevis* oocytes for two-electrode voltage clamp analysis using standard methods[29]. Currents were recorded 48 to 72 h post-injection in a bath solution containing 4 mM KCl, 85 mM NaCl, 1.8 mM $CaCl_2$ and 10 mM HEPES, pH 7.2. To record tail currents, the bath solution was switched to 89 mM RbCl, 2.4 mM $NaHCO_3$, 0.82 mM $Ca(NO_3)_2$, 0.41 mM $CaCl_2$ and 10 mM HEPES, pH 7.2. For mixing experiments, 1 ng of Kv3.3 or Shaker IR RNA was injected, in the absence or presence of the indicated ratio of mutant RNA.

Accession codes. Potassium channel, voltage-gated, Shaw-related subfamily, member 3 (KCNC3): NM_004977.

Note: Supplementary information is available on the Nature Genetics website.

ACKNOWLEDGMENTS

We thank J.L. Rae for providing the *Kv3.3* cDNA clone and T. Otis, L. Timpe and F. Schweizer for manuscript critique. Technical assistance was provided by V. Garibyan, A. Camuzat and N. Benammar. This work was supported in part by US National Institutes of Health grants to S.P. (R01N533123) and D.P. (R01GM43459, R01GM66686), a National Ataxia Foundation Grant to S.P., funding from the Programme Hospitalier de Recherche Clinique (AOMO3059) to A.D., the Verum Foundation to A.B., and the EuroSCA Integrated Project (LSHM-CT-2004-503304) to A.D., A.B. and G.S. M.F.W. is supported by the American Academy of Neurology Raymond D. Adams Fellowship in Neurogenetics. N.A.M. was supported by T32GM065823.

COMPETING INTERESTS STATEMENT
The authors declare that they have no competing financial interests.

Published online at http://www.nature.com/naturegenetics
Reprints and permissions information is available online at http://npg.nature.com/reprintsandpermissions/

1. Graves, T.D. & Hanna, M.G. Neurological channelopathies. *Postgrad. Med. J.* **81**, 20–32 (2005).
2. Herman-Bert, A. *et al.* Mapping of spinocerebellar ataxia 13 to chromosome 19q13.3-q13.4 in a family with autosomal dominant cerebellar ataxia and mental retardation. *Am. J. Hum. Genet.* **67**, 229–235 (2000).
3. Ghanshani, S. *et al.* Genomic organization, nucleotide sequence, and cellular distribution of a Shaw-related potassium channel gene, Kv3.3, and mapping of Kv3.3 and Kv3.4 to human chromosomes 19 and 1. *Genomics* **12**, 190–196 (1992).
4. Aggarwal, S.K. & MacKinnon, R. Contribution of the S4 segment to gating charge in the Shaker K^+ channel. *Neuron* **16**, 1169–1177 (1996).
5. Pulst, S.M. Inherited ataxias. in *Genetics of Movement Disorders* (ed. Pulst, S.M.) Ch. 2 (Academic, San Diego, 2003).
6. Schöls, L., Bauer, P., Schmidt, T., Schulte, T. & Riess, O. Autosomal dominant cerebellar ataxias: clinical features, genetics, and pathogenesis. *Lancet Neurol.* **3**, 291–304 (2004).
7. Waters, M.F. *et al.* An autosomal dominant ataxia maps to 19q13: allelic heterogeneity of SCA13 or novel locus? *Neurology* **65**, 1111–1113 (2005).
8. Rudy, B. & McBain, C.J. *Kv3* channels: voltage-gated K^+ channels designed for high-frequency repetitive firing. *Trends Neurosci.* **24**, 517–526 (2001).
9. Shen, N.V. & Pfaffinger, P.J. Molecular recognition and assembly sequences involved in the subfamily-specific assembly of voltage-gated K^+ channel subunit proteins. *Neuron* **14**, 625–633 (1995).
10. Long, S.B., Campbell, E.B. & MacKinnon, R. Crystal structure of a mammalian voltage-dependent *Shaker* family K^+ channel. *Science* **309**, 897–903 (2005).
11. Shieh, C.C., Klemic, K.G. & Kirsch, G.E. Role of transmembrane segment S5 on gating of voltage-dependent K^+ channels. *J. Gen. Physiol.* **109**, 767–778 (1997).
12. Smith-Maxwell, C.J., Ledwell, J.L. & Aldrich, R.W. Uncharged S4 residues and cooperativity in voltage-dependent potassium channel activation. *J. Gen. Physiol.* **111**, 421–439 (1998).
13. Seoh, S.A., Sigg, D., Papazian, D.M. & Bezanilla, F. Voltage-sensing residues in the S2 and S4 segments of the *Shaker* K^+ channel. *Neuron* **16**, 1159–1167 (1996).
14. Martina, M., Yao, G.L. & Bean, B.P. Properties and functional role of voltage-dependent potassium channels in dendrites of rat cerebellar Purkinje neurons. *J. Neurosci.* **23**, 5698–5707 (2003).
15. Matsukawa, H., Wolf, A., Matsushita, S., Joho, R. & Knöpfel, T. Motor dysfunction and altered synaptic transmission at the parallel fiber-Purkinje cell synapse in mice lacking potassium channels Kv3.1 and Kv3.3. *J. Neurosci.* **23**, 7677–7684 (2003).
16. McMahon, A. *et al.* Allele-dependent changes of olivocerebellar circuit properties in the absence of the voltage-gated potassium channels Kv3.1 and Kv3.3. *Eur. J. Neurosci.* **19**, 3317–3327 (2004).
17. McKay, B.E. & Turner, R.W. *Kv3* K^+ channels enable burst output in rat cerebellar Purkinje cells. *Eur. J. Neurosci.* **20**, 729–739 (2004).
18. Goldman-Wohl, D.S., Chan, E., Baird, D. & Heintz, N. Kv3.3b: a novel *Shaw* type potassium channel expressed in terminally differentiated cerebellar Purkinje cells and deep cerebellar nuclei. *J. Neurosci.* **14**, 511–522 (1994).
19. Weiser, M. *et al.* Differential expression of *Shaw*-related K^+ channels in the rat central nervous system. *J. Neurosci.* **14**, 949–972 (1994).
20. Espinosa, F. *et al.* Alcohol hypersensitivity, increased locomotion, and spontaneous myoclonus in mice lacking the potassium channels Kv3.1 and Kv3.3. *J. Neurosci.* **21**, 6657–6665 (2001).
21. Ruppersberg, J.P. *et al.* Regulation of fast inactivation of cloned mammalian IK(A) channels by cysteine oxidation. *Nature* **352**, 711–714 (1991).
22. Vega-Saenz de Miera, E. & Rudy, B. Modulation of K^+ channels by hydrogen peroxide (1992). *Biochem. Biophys. Res. Commun.* **186**, 1681–1687 (1992).
23. Duprat, F. Susceptibility of cloned K^+ channels to reactive oxygen species. *Proc. Natl. Acad. Sci. USA* **92**, 11796–11800 (1995).
24. McKay, B.E. & Turner, R.W. Physiological and morphological development of the rat cerebellar Purkinje cell. *J. Physiol.* **567**, 829–850 (2005).
25. Ariano, M.A. *et al.* Striatal potassium channel dysfunction in Huntington's disease transgenic mice. *J. Neurophysiol.* **93**, 2565–2574 (2005).
26. Angulo, E. *et al.* Up-regulation of the Kv3.4 potassium channel subunit in early stages of Alzheimer's disease. *J. Neurochem.* **91**, 547–557 (2004).
27. Baranauskas, G., Tkatch, T. & Surmeier, D.J. Delayed rectifier currents in rat globus pallidus neurons are attributable to Kv2.1 and Kv3.1/3.2 K(+) channels. *J. Neurosci.* **15**, 6394–6404 (1999).
28. Silverman, W.R., Tang, C.Y., Mock, A.F., Huh, K.B. & Papazian, D.M. Mg^{2+} modulates voltage-dependent activation in ether-a-go-go potassium channels by binding between transmembrane segments S2 and S3. *J. Gen. Physiol.* **116**, 663–677 (2000).
29. Rae, J.L. & Shepard, A.R. Kv3.3 potassium channels in lens epithelium and corneal endothelium. *Exp. Eye Res.* **70**, 339–348 (2000).
30. Schulteis, C.T., Nagaya, N. & Papazian, D.M. Subunit folding and assembly steps are interspersed during *Shaker* potassium channel biogenesis. *J. Biol. Chem.* **273**, 26210–26217 (1998).